Electron-lifetime effects on properties of Nb_3Sn, Nb_3Ge, and Ti-V-Cr alloys

L. F. Mattheiss and L. R. Testardi
Bell Laboratories, Murray Hill, New Jersey 07974
(Received 16 April 1979)

A simple model is applied to calculate electron-lifetime effects on the density of states, Fermi velocity, and Drude plasma energy in Nb_3Sn, Nb_3Ge, and Ti-V-Cr alloys. Formulas are provided for utilizing these results to estimate a number of superconducting and normal-state properties of these materials.

I. INTRODUCTION

Electron-lifetime effects on several basic physical parameters of some A-15 and bcc materials have recently been calculated[1] using a simple model that combines theoretical energy-band properties for perfect crystals and observed electrical resistivities. In this paper we extend these previous calculations (for V_3Si and Zr-Nb-Mo alloys) to several additional A-15 and bcc materials (Nb_3Sn, Nb_3Ge, and Ti-V-Cr alloys), and provide a catalog of formulas for applying this model to determine several superconducting and normal-state properties of these materials for arbitrary values of the resistivitiy ρ.

II. METHOD

In applying this scheme, we have used energy bands derived from a tight-binding fit to augmented-plane-wave (APW)[2] (Nb_3Sn and V) and self-consistent pseudopotential[3] (Nb_3Ge) results to calculate the density of states $N(E)$, Fermi velocity $v_F(E)$, and Drude plasma energy $\Omega_p(E)$ for the perfectly ordered materials. Electron-lifetime effects are introduced by averaging these quantities over an energy interval $E_B = \hbar/\bar{\tau}$ about the Fermi level. The mean electron lifetime $\bar{\tau}$ is estimated by combining the calculated plasma energy $\langle\Omega_p^2\rangle^{1/2}$ (lifetime averaged) and the observed electrical resistivity ρ, using

$$\rho^{-1} = \frac{\langle\Omega_p^2\rangle\bar{\tau}}{4\pi\hbar^2} . \tag{1}$$

To test the sensitivity of the results to the detailed shape of the broadening function, both Lorentzian and Fermi-Dirac (with $T = T_B \equiv \hbar/k\bar{\tau}$) functions have been used.[1] These yield results which agree to within $\lesssim$10%, which is the estimated accuracy of this method. Finally, we expect these calculated lifetime effects to apply equally to both thermal and defect resistivities at room temperature and below since $T_B >> T$ for the materials considered here.

III. RESULTS

Figures 1, 2, and 3 show the lifetime-averaged values of the bare density of states, Fermi velocity, and Drude plasma energy for Nb_3Sn and $Nb_{2.93}Sn$, Nb_3Ge, and a series of Ti-V-Cr bcc alloys. These results use the Fermi-Dirac form of broadening function. The large differences in the calculated $\langle N\rangle$ and $\langle v_F\rangle$ at low ρ for $Nb_{3-x}Sn$ in Fig. 1 reflect details in the tight-binding interpolation scheme band structure[2] which we regard as unreliable. Experimental evidence indicates a high value for N in the low-ρ state. For $\rho \gtrsim 30\ \mu\Omega$ cm, however, the lifetime-averaged values are similar.

By using the thermal resistivity $\rho(T)$ for the ordinates of Figs. 1, 2, and 3 (and Figs. 1 and 2 of Ref. 1), one obtains, implicitly, the temperature dependence of $\langle N\rangle$, $\langle v_F\rangle$, and $\langle\Omega_p^2\rangle^{1/2}$ resulting from lifetime broadening. (For example, at 300 K $\rho \sim 70$–$80\ \mu\Omega$ cm for A-15 compounds.) These large variations, which are at least qualitatively in agreement with experiment for the A-15 compounds and Nb (we are unaware of data for V), result from fine structure in the calculated $N(E)$ results on a scale of 50–100 meV. This is in contrast to the fine structure of several meV sometimes invoked in theories of the A-15's to explain these temperature dependences. The importance of the lifetime broadening, compared to the thermal broadening used in the model theories, is quickly seen by comparing T_B (see Figs. 1–3) with T.

We present below a short list of formulas by which a number of important physical parameters can be obtained in terms of the calculated quantities. To simplify their use, practical units have been employed and these are listed following the equations. The definitions with proper units are given in parentheses.

The mean free path is given by

$$l = v_F\tau = \frac{4.91\times10^4 v_F}{\Omega_p^2\rho} . \tag{2}$$

The relaxation time is given by

$$\tau = l/v_F = \frac{4.91\times10^{-12}}{\Omega_p^2\rho} . \tag{3}$$

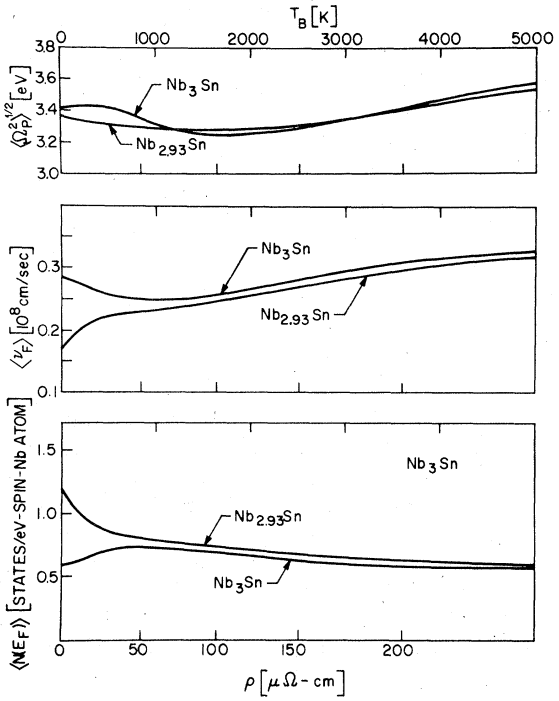

FIG. 1. Density of states $\langle N\rangle$, Fermi velocity $\langle v_F\rangle$, and Drude plasma energy $\langle\Omega_p^2\rangle^{1/2}$ as a function of resistivity for Nb_3Sn and $Nb_{2.93}Sn$.

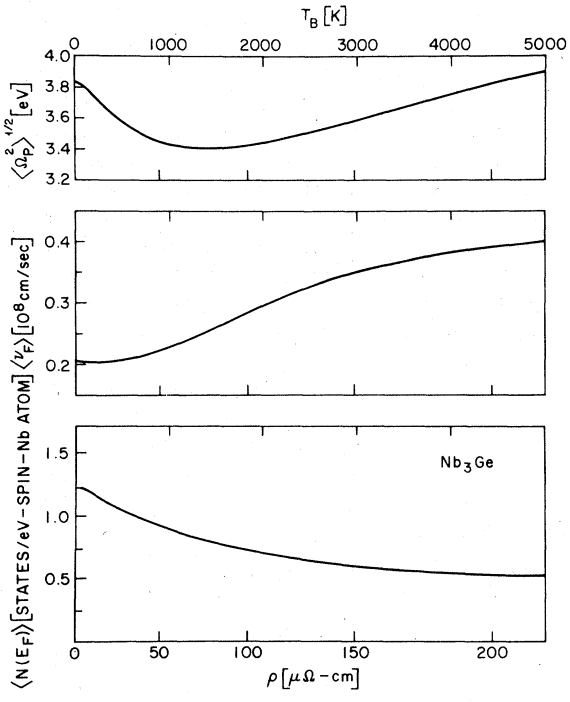

FIG. 2. Density of states $\langle N\rangle$, Fermi velocity $\langle v_F\rangle$, and Drude plasma energy $\langle\Omega_p^2\rangle^{1/2}$ as a function of resistivity for Nb_3Ge.

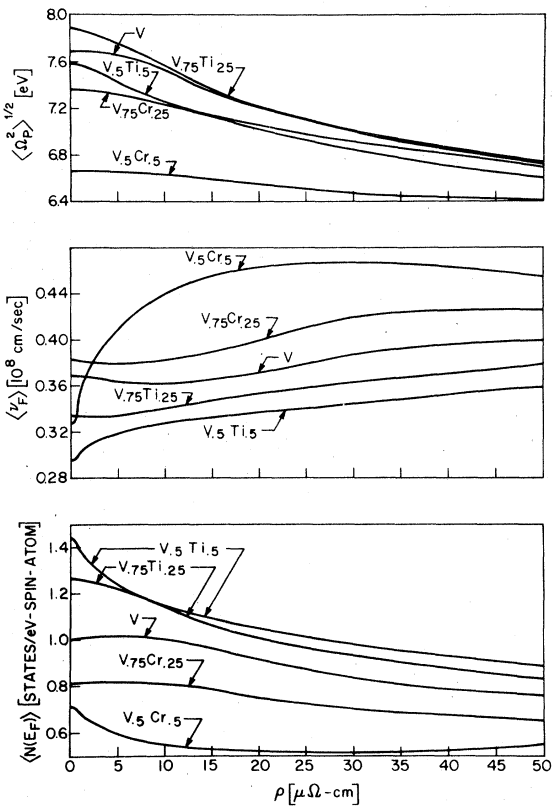

FIG. 3. Density of states $\langle N\rangle$, Fermi velocity $\langle v_F\rangle$, and Drude plasma energy $\langle\Omega_p^2\rangle^{1/2}$ as a function of resistivity for Ti-V-Cr bcc alloys.

The broadening temperature is given by

$$T_B = \hbar/k\bar{\tau} = 1.554\,\Omega_p^2\rho\ . \tag{4}$$

The BCS coherence length[4,5] at 0 K is given by

$$\xi_0^*(0) = \left(\frac{0.18\,\hbar v_F^*}{kT_c}\right) = \frac{1.38\times10^4 v_F}{(1+\lambda)T_c}\ . \tag{5}$$

The London penetration depth[4,5] at 0 K is given by

$$\lambda_L^*(0) = \left(\frac{c\,\hbar}{\Omega_p}\right) = \frac{1.98\times10^3(1+\lambda)^{1/2}}{\Omega_p}\ . \tag{6}$$

The Ginzburg-Landau κ near T_c is[5]

$$\kappa^* = \frac{0.137(1+\lambda)^{3/2}T_c\eta_{H_{c2}}}{\Omega_p v_F \chi(Z)} \tag{7}$$

and the temperature dependence of the upper critical field near T_c is given by[5]

$$\left.\frac{-dH_{c2}}{dT}\right|_{T_c} = \frac{3.18(1+\lambda)^2T_c\eta_{H_{c2}}}{\chi(Z)v_F^2}\ , \tag{8}$$

where

$$Z = \frac{0.88\xi_0^*(0)}{l} = \frac{0.246\,\Omega_p^2\rho}{(1+\lambda)\,T_c} \tag{9}$$

and

$$\chi(Z) = \frac{\sum_{\nu=0}^{\infty}(2\nu+1)^{-2}(2\nu+1+Z)^{-1}}{\sum_{\nu=0}^{\infty}(2\nu+1)^{-3}} . \tag{10}$$

One may approximate χ by

$$\chi_a(Z) = \left(1+\frac{Z}{1.173}\right)^{-1} , \tag{11}$$

which is exact in the clean $[\xi_0(0)/l \to 0]$ and dirty $[\xi_0(0)/l \to \infty]$ limits and makes a maximum error of ~6% (χ_a too large) at Z between 2 and 3. In the dirty limit

$$\left.\frac{-dH_{c2}}{dT}\right|_{T_c}^{\text{dirty}} = \frac{3.49\times10^3(1+\lambda)N\rho\eta_{H_{c2}}}{a_0^3} . \tag{12}$$

Finally, Ω_p, N, and v_F are related by

$$\Omega_p^2 = \left(\frac{8\pi}{3}\hbar^2e^2v_F^2N\right) = \frac{5.24\times10^3v_F^2N}{a_0^3} . \tag{13}$$

Units and definitions. N [states/(spin eV unit-cell)] ("bare"). (The calculated N's in Figs. 1–3 are per transition-metal atom.) v_F (10^8 cm/sec) ("bare"). l, $\xi_0^*(0)$, λ_L^*, and a_0 in (Å). a_0^3 is the volume of the unit cell (Å^3). ρ_0 ($\mu\Omega$ cm); Ω_p (eV); dH_{c2}/dT (oersteds/K). $\eta_{H_{c2}}$ is the strong-coupling correction of Rainer and Bergman.[6] ($\eta_{H_{c2}}=1$ for weak coupling and ~1.25 for $T_c/\langle\omega\rangle=0.1$). λ is the electron-phonon renormalization parameter. Equations (2)–(13) are evaluated with the lifetime-broadened parameters, $\langle\Omega_p^2\rangle^{1/2}$, $\langle v_F\rangle$, and $\langle N\rangle$, respectively.

Tables I and II summarize some calculated properties of these A-15 and bcc materials which are derived from Eqs. (2)–(13) for representative values of ρ.[7] For the A-15 materials the lower chosen values of ρ are typical of "as-grown" materials at low temperatures while the higher value (150 $\mu\Omega$ cm) is about twice the room-temperature resistivity and is characteristic of the "saturated defect state".[8] For Nb and V the lower and higher ρ's correspond to residual resistivities of clean materials at low T, and to thermal resistivities (very roughly) at 300 K, respectively. Typical residual resistivities have been chosen for $Nb_{0.5}Zr_{0.5}$ and $Nb_{0.5}Mo_{0.5}$.

The calculated quantities in Tables I and II include electron-phonon renormalization where applicable,

TABLE I. Calculated properties of A-15 compounds.

	V_3Si		Nb_3Sn		Nb_3Ge	
ρ ($\mu\Omega$ cm)	3.75	150	10	150	40	150
τ^* (10^{-14} sec)	$11.2(1+\lambda)$	$0.30(1+\lambda)$	$4.35(1+\lambda)$	$0.30(1+\lambda)$	$1.0(1+\lambda)$	$0.25(1+\lambda)$
l (Å)	160–190	7.7	90–120	8.7	21	8.8
$\xi_0^*(0)$ (Å)	$\frac{115-140}{1+\lambda}$	$\frac{1630}{1+\lambda}$	$\frac{95-130}{1+\lambda}$	$\frac{810}{1+\lambda}$	$\frac{79}{1+\lambda}$	$\frac{864}{1+\lambda}$
$\xi_d^*(0)\equiv(\xi_0^*l)^{1/2}$ (Å)	...	$\frac{112}{(1+\lambda)^{1/2}}$	...	$\frac{84}{(1+\lambda)^{1/2}}$	...	$\frac{87}{(1+\lambda)^{1/2}}$
$\lambda_L^*(0)$ (Å)	$584(1+\lambda)^{1/2}$	$598(1+\lambda)^{1/2}$	$585(1+\lambda)^{1/2}$	$603(1+\lambda)^{1/2}$	$565(1+\lambda)^{1/2}$	$549(1+\lambda)^{1/2}$
$\lambda_d(0)\equiv\lambda_L^*(0)\left(\frac{\xi_0^*}{l}\right)^{1/2}$ (Å)	...	8700	...	5820	...	5440
$\kappa^*/\eta_{H_{c2}}$	$(4-5)(1+\lambda)^{3/2}F^a$	$57(1+\lambda)^{1/2}$	$(4.3-5.9)(1+\lambda)^{3/2}F^a$	$52(1+\lambda)^{1/2}$	$7(1+\lambda)^{3/2}F^a$	$46(1+\lambda)^{1/2}$
$\eta_{H_{c2}}^{-1}\left.\frac{-dH_{c2}}{dT}\right\|_{T_c}\left(\frac{\text{kOe}}{\text{K}}\right)$	$(2-2.8)(1+\lambda)^2F^a$	$21(1+\lambda)$	$(0.8-1.4)(1+\lambda)^2F^a$	$14(1+\lambda)$	$1.7(1+\lambda)^2F^a$	$13(1+\lambda)$
T_c (K)	17	2.2	18	3.0	23	3.5

[a] $F\equiv1+C/(1+\lambda)$, where $C=0.54$, 1.33, and 4.7 for V_3Si, Nb_3Sn, and Nb_3Ge, respectively.

TABLE II. Calculated properties of bcc materials.

	Nb		$Nb_{0.5}Zr_{0.5}$	$Nb_{0.5}Mo_{0.5}$	V	
ρ ($\mu\Omega$ cm)	≈ 0	15	40	15	≈ 0	25
τ^* (10^{-14} sec)	...	$0.44(1+\lambda)$	$0.20(1+\lambda)$	$0.55(1+\lambda)$	...	$0.39(1+\lambda)$
l (Å)	...	27.4	10.8	41.4	...	13.6
$\xi_0^*(0)$ (Å)	$\frac{840}{1+\lambda}$	$\frac{1300}{1+\lambda}$	$\frac{828}{1+\lambda}$	$\frac{1.5\times10^5}{1+\lambda}$	$\frac{833}{1+\lambda}$	$\frac{2420}{1+\lambda}$
$\xi_d^*(0) \equiv (\xi_0^* l)^{1/2}$ (Å)	...	$\frac{189}{1+\lambda}$	$\frac{94.6}{(1+\lambda)^{1/2}}$	$\frac{2490}{(1+\lambda)^{1/2}}$	...	$\frac{181}{(1+\lambda)^{1/2}}$
$\lambda_L^*(0)$ (Å)	$222(1+\lambda)^{1/2}$	$230(1+\lambda)^{1/2}$	$252(1+\lambda)^{1/2}$	$255(1+\lambda)^{1/2}$	$257(1+\lambda)^{1/2}$	$279(1+\lambda)^{1/2}$
$\lambda_d(0) \equiv \lambda_L^* \left(\frac{\xi_0^*}{l}\right)^{1/2}$ (Å)	...	1585	2210	1.54×10^4	...	3720
$\kappa^*/\eta_{H_{c2}}$	$0.25(1+\lambda)^{3/2}$	$7(1+\lambda)^{1/2}$	$16.7(1+\lambda)^{1/2}$	$5.2(1+\lambda)^{1/2}$	$0.30(1+\lambda)^{3/2}$	$14.6(1+\lambda)^{1/2}$
$\eta_{H_{c2}}^{-1} \frac{-dH_{c2}}{dT}\Big\vert_{T_c}$ $\left(\frac{\text{kOe}}{\text{K}}\right)$	$0.09(1+\lambda)^2$	$2.3(1+\lambda)$	$5.6(1+\lambda)$	$0.07(1+\lambda)$	$0.17(1+\lambda)^2$	$6,85(1+\lambda)$
T_c (K)	9.2	~6.6	9.0	0.07	5.3	~2.0

and the renormalization factor is explicitly shown. Strong-coupling corrections are given only for κ^* and $(-dH_{c2}/dT)_{T_c}$. For several A-15 materials, a range of values is given for the low-ρ state. These reflect our estimate of the uncertainties in the calculated fine structure in $N(E)$ and $v_F(E)$ which originate from inaccuracies in the tight-binding fit to the APW results as well as the APW bands themselves.

In general, the results in Tables I and II are less reliable for the low-ρ state. Independent APW band-structure calculations[9,10] utilizing more precise interpolation techniques indicate that larger values of $N(E_F)$ and smaller values of v_F are appropriate for Nb_3Sn. Similar discrepancies also occur in Nb_3Ge where two independent calculations[3,9] yield values of $N(E_F)$ which differ by a factor of 2.

For all materials high ρ is accompanied by a reduced λ and T_c. The values chosen for the latter (see Tables I and II) in calculating the superconducting properties are experimental, but they are also consistent with those calculated from lifetime-broadened properties.[1] All calculations can be extended to any value of ρ, of course, using Eqs. (2)–(13) above, and Figs. 1 to 3 of this paper and Figs. 1 and 2 of Ref. 1.

Note that typical as-grown A-15 compounds (see values in the low-ρ columns of Table I) do not well satisfy the clean limit approximation $l \gg \xi_0$. Therefore, in these materials the coherence length will be somewhat different from ξ_0, and the field penetration depth will be somewhat greater than λ_L, at absolute zero. The saturated defect state, however, is well described by the dirty limit approximation $l \ll \xi_0$ so that ξ_d and λ_d are appropriate. However, due to the unusually large changes in v_F, T_c, and λ with increasing ρ one obtains in A-15's the unusual result that ξ_d (high ρ) is not much different than ξ_0 (low ρ) and should, in fact, be larger than ξ_0 (low ρ).

Accurate values for λ are not known in most cases. For V_3Si estimates range from $\lambda \sim 0.8$–0.9 (specific heat and magnetic susceptibility[11]) to $\lambda \sim 1.29$ (α^2F measurements by far infrared transmission[12]) for low-ρ material. From tunneling (α^2F measurements) the values $\lambda \sim 1.67$ for Nb_3Sn,[13] and $\lambda \sim 0.95$ for Nb,[14] have been reported for the low-ρ materials. Significant reductions in λ occur in the high-ρ states with λ in the A-15 saturated defect state probably being $\sim\frac{1}{2}$ its value in the low-ρ state.[1,8,11] The strong-coupling correction[6] $\eta_{H_{c2}}$ probably lies between 1 and 1.35 for the materials considered here.

ACKNOWLEDGMENT

We are grateful to W. E. Pickett for sending us a preliminary version of Ref. 3.

---

[1]L. R. Testardi and L. F. Mattheiss, Phys. Rev. Lett. 41, 1612 (1978). We note that a factor of $\hbar^2$ was omitted from Eq. (2) of this paper.

[2]L. F. Mattheiss, Phys. Rev. B 12, 2161 (1975); L. F. Mattheiss, L. R. Testardi, and W. W. Yao, Phys. Rev. B 17, 4640 (1978). The present energy-band results for V are derived from unpublished APW calculations.

[3]W. E. Pickett, K. M. Ho, and M. L. Cohen, Phys. Rev. B 19, 1734 (1979).

[4]For $t \equiv T/T_c \sim 1$ the penetration depth

$$\lambda = \frac{\lambda_L(0)}{\sqrt{2}} \frac{(1-t)^{-1/2}}{\chi^{1/2}(Z)}$$

and the coherence length $\xi = \lambda/\kappa$. For $t \to 0$ in the dirty limit $\lambda \to \lambda_L(\xi_0/l)^{1/2}$ and $\xi \to (\xi_0 l)^{1/2}$.

[5]See, for example, A. Fetter and P. C. Hohenberg, in *Superconductivity,* edited by R. D. Parks (Marcel Dekker, New York, 1969), Vol. 2.

[6]D. Rainer and G. Bergman, J. Low Temp. Phys. 14, 501 (1974). We have assumed that these strong-coupling corrections apply in the clean as well as the dirty limits.

[7]For V_3Si, $\rho_0 = 3.75\ \mu\Omega$ cm corresponds to a resistance ratio (RR) of ~20 which is the approximate dividing line between nontransforming (RR less than 20) and transforming crystals. The equivalent lifetime broadening temperature for RR =20 is $T_B \sim 50$ K which is roughly 2.5 times the structural transformation temperature $T_m \sim 21$ K. Thus, as pointed out by S. J. Williamson, C. S. Ting, and H. K. Fung [Phys. Rev. Lett. 32, 9 (1974)], the lifetime-broadening effects are very important for the structural transformation.

[8]R. Viswanathan and R. Caton, Phys. Rev. B 18, 15 (1978).

[9]B. M. Klein, L. L. Boyer, D. A. Papconstantopoulos, and L. F. Mattheiss, Phys. Rev. B 18, 6411 (1978).

[10]A. T. van Kessel, H. W. Myron, and F. M. Mueller, Phys. Rev. Lett. 41, 181 (1978).

[11]A. Guha, M. P. Sarachik, F. W. Smith, and L. R. Testardi, Phys. Rev. B 18, 9 (1978).

[12]S. McKnight, S. Perkowitz, D. Tanner, and L. R. Testardi Phys. Rev. (to be published).

[13]L. Y. L. Shen, Phys. Rev. Lett. 29, 1082 (1972).

[14]P. B. Allen and R. C. Dynes, Phys. Rev. B 12, 905 (1975).